

Role of TELO2-interacting protein 1(TTI1) functions as an oncogene by regulating mTOR activity in the progression of non-small cell lung cancer

Ling-Xian Zhang

Department of Cardiothoracic Surgery, the Second Affiliated Hospital of Nanchang University

Xin Yang

Department of Cardiothoracic Surgery, the Second Affiliated Hospital of Nanchang University

Zhi-Bo Wu

Department of Cardiothoracic Surgery, the Second Affiliated Hospital of Nanchang University

Zhong-Min Liao

Department of Cardiothoracic Surgery, the Second Affiliated Hospital of Nanchang University

Ding-Guo Wang

Department of Cardiothoracic Surgery, the Second Affiliated Hospital of Nanchang University

Shi-Wei Chen

Department of Cardiothoracic Surgery, the Second Affiliated Hospital of Nanchang University

Feng Lu

Department of Cardiothoracic Surgery, the Second Affiliated Hospital of Nanchang University

Yong-Bing Wu

Department of Cardiothoracic Surgery, the Second Affiliated Hospital of Nanchang University

Shu-Qiang Zhu (✉ zsqs276446377@163.com)

Department of Cardiothoracic Surgery, the Second Affiliated Hospital of Nanchang University

Research Article

Keywords: TELO2-interacting protein 1(TTI1), NSCLC, mTOR, KI67

Posted Date: April 8th, 2022

DOI: <https://doi.org/10.21203/rs.3.rs-1522047/v1>

License:   This work is licensed under a Creative Commons Attribution 4.0 International License.

[Read Full License](#)

Abstract

Background: The role of TTI1 in the progression of several types of cancer has been reported recently. The aim of this study was to estimate the expression and the potential value of TTI1 in non-small cell lung cancer (NSCLC) patients.

Methods: The expression of TTI1 and its prognostic value in NSCLC from The Cancer Genome Atlas (TCGA) database and Gene Expression Omnibus (GEO) database were analyzed. To verify the bioinformatics findings, a tissue microarrays (TMAs) containing 160 NSCLC and paired peritumoral tissues from NSCLC patients was analysed by immunohistochemistry for TTI1. Subsequently, the roles of TTI1 in NSCLC cells were investigated in vivo by establishing xenograft models in nude mice, and in vitro by transwell, CCK-8 assay, wound healing and colony formation assays. In addition, qRT-PCR and western blot were applied to explore the underlying mechanism by which TTI1 promotes tumor progression. Finally, the relation between TTI1 and Ki67 expression level of NSCLC was probed, and Kaplan-Meier and Cox's analyses were performed to assess the prognostic merit of TTI1 and Ki67 in NSCLC patients.

Results: The expression of TTI1 was significantly upregulated in NSCLC tissues compared to paired peritumoral tissues, which was coincide with the bioinformatics findings from TCGA and GEO database. TTI1 was highly expressed in NSCLC patients with large tumor, advanced tumor stage, and lymphatic metastasis. In addition, the prognostic analysis identified the TTI1 as an independent indication for poor prognosis of NSCLC patients. In vitro, Up-regulation of TTI1 in NSCLC cells could facilitate cell invasion, metastasis, viability and proliferation. Mechanistically, our study verified that TTI1 could regulate mTOR activity which has a pivotal role in human cancer. Consistently, the TTI1 and Ki67 expression had a positive relationship in NSCLC cells and tissues. Notably, compared with patients with low expression of TTI1 or Ki67, patients with overexpression of TTI1 or Ki67 had a shorter overall survival rate (OS) and a higher disease-free survival rate (DFS), and the combination of TTI1 and Ki67 was an independent parameter predicting the prognosis and recurrence of NSCLC patients.

Conclusions: TTI1 promotes NSCLC cell proliferation, metastasis and invasion by regulating mTOR activity and the combination of TTI1 and Ki67 is a valuable molecular biomarker for the survival and recurrence of NSCLC patients.

Background

Lung cancer remains one of the most frequent malignancies and is the leading cause of cancer-related deaths worldwide [1]. NSCLC is the major pathological type of lung cancer, accounting for about > 80% of the whole cohort[2]. Despite much progress has been made recently for NSCLC, such as minimally invasive techniques for diagnosis and treatment, targeted therapies, and immunotherapies, the overall 5-year survival rate of all NSCLC patients only approximately 15% and most postoperative patients may have early tumor recurrence [3]. Thus, further investigation on the mechanism associated with cancer progression and recurrence is extremely urgent.

TELO2-interacting protein 1 (TTI1), also known as KIAA0406 or SMG10, is a member of TTT complex that is composed of TELO2, TTI1, and TTI2[4]. TTI1 is highly conserved throughout evolution and has homology in mice, chickens, flies, frogs, fish, plants and yeast. TTT complex works synergistically with HSP90 to maintain the function of the phosphatidylinositol 3-kinase-related protein kinase (PIKK) family proteins[5]. Mammalian target of rapamycin (mTOR), a serine/threonine kinase and a member of the phosphatidylinositol 3-kinase-related kinase (PIKK) family, regulates translation, cell growth, and autophagy, etc, and has a pivotal role in human cancer[6]. TTI1 is a mTOR-interacting protein, that interacts with and stabilizes all six members of the PIKK family of proteins (mTOR, ATM, ATR, DNA-PKcs, SMG-1, and TRRAP)[7]. TTI1 participates in important biological functions. TTI1 and its binding partner Tel2 positively Regulates mTOR Activity and involves in cell growth and metabolism[7]. TTI1 via its C-terminus binds with IP6K2 and participates in the signaling pathway of p53-associated cell death mediated by IP6K2[8]. In multiple myeloma, SCFFbxo9 target Tel2 and Tti1 for degradation within mTORC1 and mTORC1 is inactivated to restrain cell growth and protein translation[9]. As mentioned above, TTI1 may be involved in oncogenesis and progression of NSCLC, and further study is necessary.

In this study, we analyzed TTI1 expression and its prognostic value within NSCLC patients by using bioinformatics method. Then, a tissue microarrays (TMAs) was analysed to verify the bioinformatics findings that TTI1 was significantly upregulated in NSCLC tissues and is closely associated with the poor prognosis of NSCLC patients. Additionally, we identified that TTI1 could promote the progression of NSCLC. Mechanistically, our study verified the regulation of mTOR signaling pathway by TTI1. Subsequently, the relationship between the expression of TTI1 and/or Ki67 and the clinicopathological characteristics of NSCLC patients was further studied. Finally, we analyzed the relationship between the expression of TTI1 and Ki67 and the prognosis and recurrence of NSCLC patients.

Methods

Expression data sets

Seven human lung cancer cohorts and corresponding clinical information were extracted from the Gene Expression Omnibus (GEO; GSE19188, GSE40791, GSE75037, GSE41271, GSE50081 and GSE31210) and The Cancer Genome Atlas (TCGA) database to analyze the expression of TTI1.

Patients and following-up

A total of 160 NSCLC tissues and matched nontumor tissues were gathered from patients who underwent surgery at the Second Affiliated Hospital of Nanchang University. The pathological diagnosis was carried out by two pathologists respectively in accordance with the standards of the World Health Organization. Those tissues were constructed into a tissue microarray (TMA) that was used to perform immunohistochemistry (IHC) staining. Clinicopathological information was collected from 12 March 2009 to 28 February 2011. The last follow-up was in December 2019. All patients had written informed consent regarding the collection and use of their tissue samples. The ethical approval was authorized by the Second Affiliated Hospital of Nanchang University.

Tissue Microarray establishment and Immunohistochemistry

Tissue microarrays (TMAs) of 160 pairs of NSCLC tissues and matched nontumor tissues were built by Shanghai Biochip Co, Ltd (Shanghai, China). Rabbit polyclonal to human TTI1 antibody (1:200, ab234871, Abcam, USA) and Rabbit polyclonal to human Ki67 antibody (1:200, ab16667, Abcam, USA) were used to detect the expression of TTI1 and Ki67. The immunohistochemistry (IHC) assay was performed according to a standard protocol. In brief, after baking at 37°C for 30 minutes, all paraffin sections of the human lung cancer tissues were first dewaxed and then rehydrated. 5% bovine serum albumin (BSA) (YESEN, Shanghai, China) was incubated for 1 h at room temperature to block nonspecific binding sites. Then, the sections were incubated with primary antibodies overnight at 4°C. Subsequently, endogenous peroxidase activity was blocked with incubation of the slides in 0.3% H₂O₂ at room temperature for 30 min, followed by incubation with secondary antibody for 1 h at room temperature. Next, the sections were stained with diaminobenzidine (DAB)-H₂O₂ (Gene Tech, Shanghai, China) under a microscope and counterstained with hematoxylin. Finally, neutral balsam (Yeasen, Shanghai, China) was used to seal the slides with a cover slip. All assays included Negative control slides without the primary antibodies. TTI1 staining was seen mainly in the cytoplasm of NSCLC and Ki67 was usually seen in the nucleus. Histochemistry score (H-score) was defined as the score for staining intensity multiplying with the score for staining percentage. According to the average intensity, the intensity was scored as follows: score 0: negative (0-25%), score 1: weak (≥25%-50%), score 2: moderate (≥50%-75%) and score 3: strong (≥75%). Based on the percentage of positive tumor cells, the percentage was scored as follows: score 1: negative (0-25%), score 2: weak (≥25%-50%), score 3: moderate (≥50%-75%) and score 4: strong (≥75%).

Cell culture

The cell lines involved in this study included the human NSCLC cell lines A549, PC-9, NCI-H460, NCI-H1299 and the human bronchial epithelioid cell HBE, which were obtained from the Cell Bank of the Chinese Academy of Sciences (Shanghai, China). The cells were cultivated in DMEM or RPMI-1640 (Gibco, USA) supplemented with 10% fetal bovine serum (Gibco, USA) and 1% penicillin-streptomycin (Yeasen, Shanghai, China). The environment conditions were 37°C and 5% CO₂ in a humidified incubator.

Total RNA extraction and qRT-PCR detection

Total RNA from cultured cells was extracted using Trelief™ RNAprep FastPure Tissue Cell Kit (Tsingke, Beijing, China) and reverse transcribed into cDNA using a Hifair® III 1st Strand cDNA Synthesis Kit (gDNA digester plus) (Yeasen, Shanghai, China) according to the manufacturer's instructions. Subsequently, according to the manufacturer's protocol, quantitative real-time polymerase chain reaction (qRT-PCR) was performed with Hieff® qPCR SYBR Green Master Mix (High Rox Plus) (Yeasen, Shanghai, China). Glyceraldehyde-3-phosphate dehydrogenase (GAPDH) was used as an internal reference gene for quantification of mRNA. The relative RNA level was calculated by using the 2^{-ΔΔCt} method. The RT-qPCR primers used in this study are as follows, TTI1, Forward primer: AAGTCATGCTGCGGAACTCA, Reverse

primer: TGGGAACCACTGGGCTAATG; mTOR, Forward primer: CCAGGCCGCATTGTCTCTAT, Reverse primer: AGTCTCTAGCGCTGCCTTTC; S6K1, Forward primer: CTGAGGACATGGCAGGAGTG, Reverse primer: ACAATGTTCCATGCCAAGTTCA. EIF4EBP1 Forward primer: CAAGGGATCTGCCACCATT, Reverse primer: AACTGTGACTCTTCACCGCC. All experiments were done three times.

Transfection experiment

The lentiviral vectors of TTI1 and shTTI1 were obtained from Genomeditech (Shanghai, China) to construct stably transfected cell lines. The three shRNA target sequences respectively is 5'-GCAGAACAGGAGAAATCAAAG-3', 5'-GGTCACAGCATTGTCGTATCT-3' and 5'-GCAAGCTGCCATGATCCTTAA-3'. The transfection efficiency was examined by western blotting and qRT-PCR.

Colony formation and Cell Counting Kit-8 (CCK-8) assay

The colony formation and the CCK-8 assay were employed to determine the cellular proliferation. For colony formation assay, 1000 cells per well were cultured in a 6-well plate (Corning, NY, USA) for 10 days. Then, all wells were rinsed with phosphate-buffered saline (PBS) three times, fixed with 4% paraformaldehyde for 10 minutes, and stained with 0.4% crystal violet for 15 minutes. After rinsing with water and drying, all wells were photographed, and the total number of colonies was observed and counted. The results of three independent experiments were shown as mean \pm standard deviation. For the CCK-8 assay, the Cell Counting Kit-8 (CCK-8, Yeasen, Shanghai, China) was purchased and performed according to the manufacturer's protocol. Firstly, seeded cells in a 96-well plate (Corning, NY, USA) approximately at 1000 cells/well, Then, 10 μ l of CCK-8 reagent was added to each well after 24, 48, and 72h; the plates were incubated for 2h; and the absorbance of all plates was measured at 450 nm.

Wound healing, migration and transwell invasion assays

The wound healing assay and transwell assay (with Matrigel coating) were performed to detect cell invasion. For wound healing assay, seeded cells in a 6-well plate (Corning, NY, USA) and cultured until confluent. Then, using a (yellow) pipette tip made a straight scratch, simulating a wound. Subsequently, the cells were photographed at 0, 24 and 48h. For transwell assay (with Matrigel coating) (BD Biosciences, Franklin Lakes, NJ), first, placed Matrigel coating into the upper chamber and then, 1×10^6 cells in serum-free medium were seeded into it. 500 μ l culture medium containing 10% FBS was added into under chamber. After incubation for 36 h at 37 °C in a humidified atmosphere of 5% CO₂, the transwell chambers was fixed with 4% paraformaldehyde for 10 minutes and stained with 0.4% crystal violet for 15 minutes. Finally, the transwell chambers was rinsed and the upper cell layer from the filter was wiped with a cotton swab, and the cells were photographed under a microscope and counted.

Western blot analysis

The procedures of the experiments were performed according to previous studies [10, 11]. In brief, cells were lysed with RIPA buffer (Beyotime, China) containing PMSF (Beyotime, China). The cell lysates were collected and centrifuged for 15 min at 12,000g (4°C). The supernatants were transferred to clean tubes,

and SDS-PAGE sample loading buffer (Beyotime,China) was added. Then, they were boiled for 10 min and cooled down to room temperature. Proteins were subsequently separated on SDS-PAGE electrophoresis and then transferred onto polyvinylidene fluoride (PVDF) membranes (Millipore, USA). The membranes were blocked with protein free rapid blocking buffer (Epizyme, China) and incubated overnight at 4°C with primary antibodies. At the following day, the membranes were incubated with an HRP-conjugated secondary antibody for 1h at room temperature and visualized by super ECL detection reagent (Yeasen, Shanghai, China) according to the manufacturer's instructions. The TTI1 (1:5000, ab176696, Abcam, USA), p-mTOR(1:1000, ab109268, Abcam, USA), mTOR(1:5000, ab134903, Abcam, USA), p-S6K1 (1:1000, ab228513, Abcam, USA), S6K1(1:1000, ab32359, Abcam, USA),p-4EBPI (1:1000, ab27792, Abcam, USA), 4EBP1(1:2000, ab32024, Abcam, USA), Tublin (1:1000, AF0001, Beyotime, China) and GAPDH (1:1000, AF0006, Beyotime, China) was used as primary antibodies.

In vivo tumor growth

Immunodeficient nude mice (4-6 weeks of age) were purchased from Jiesijie (Shanghai, China) and fed in a pathogen-free environment. The experiment was approved by the Animal Experimentation Ethics Committee of the Second Affiliated Hospital of Nanchang University. About 5×10^6 cells were resuspended in 150 μ l DMEM and injected subcutaneously into the right side of the flank area of nude mice. Tumor volumes were calculated $(\text{length} \times \text{width}^2)/2$ every four days.

Statistical analysis

The SPSS 23.0 software program (IBM SPSS, Chicago, IL, USA) was used for statistical calculations. The values were showed as the mean \pm standard deviation. The chi-squared or Fisher's exact tests was used to compare the categorical variables and the Student's t test was chosen to compare difference of measurement data between two groups. Spearman correlation analysis was used to detect correlation between the expression of TTI1 and KI67. The best cut-off value of TTI1 and KI67 expression was divided by X-tile software[12]. The overall survival (OS) and disease-free survival (DFS) analyses were estimated by the Kaplan-Meier method, and the comparison was evaluated by the log-rank test. The univariate and multivariate analyses were conducted using a model of Cox's proportional hazards regression. $P < 0.05$ was regarded as statistically significant.

Results

Expression of TTI1 mRNA was significantly upregulated and high level of TTI1 mRNA predicts unfavorable prognosis in NSCLC

Compared to normal lung tissues, TTI1 mRNA expression was significantly upregulated in LUAD and LUSC (Fig. 1A) based on TCGA analysis, and a similar result was discovered in three independent GEO NSCLC cohorts (Fig. 1B). Furthermore, we founded that there was a significant positive correlation between the TTI1 mRNA and advanced TNM stage (Fig. 1C). The expression of TTI1 mRNA in patients with recurrence was significantly higher than those without (Fig. 1D). To investigate the prognostic value

of TTI1 mRNA, we analyzed the overall survival (OS), First progression (FP) and Post progression survival (PPS) rates in the GEO NSCLC cohort and two additional independent GEO cohorts (GSE50081 and GSE31210). Kaplan-Meier analysis showed that the OS, FP and PPS time of patients with high expression of TTI1 mRNA was significantly shorter than that of patients with low expression of TTI1 mRNA in almost all NSCLC cohort (Fig. 1E-J). The same result (overall survival) was verified in TCGA LUAD and LUSC cohorts (Fig. 1K). Overall, these results indicated that TTI1 mRNA was significantly upregulated and may represent a new prognostic biomarker for NSCLC patients.

TTI1 protein levels was also upregulated and positively associated with tumorigenic phenotypes of NSCLC patients

Furthermore, TMAs of 160 pairs of NSCLC tissues and matched nontumor tissues were used to validate the dysregulated TTI1 expression in NSCLC at protein level. The results exhibited that the expression of TTI1 in NSCLC tissues was significantly higher than that in non-cancerous tissues (Fig. 2A). Moreover, we found that high TTI1 expression was significantly correlated with larger tumor size, advanced TNM stage and lymph node metastasis (Fig. 2B-D). The TTI1 protein was mostly located in cytoplasm (Fig. 2E). The X-tile software was used to divide the best cutoff value to distinguish TTI1^{high} and TTI1^{low} groups of 160 NSCLC specimens. As shown in Table 1, TTI1^{high} was significantly correlated with larger tumor size (P = 0.003), advanced TNM stage (P=0.008), lymph node metastasis (P = 0.043) and poor differentiation (P = 0.039). while the other clinical characteristics, including age, gender, smoking history, histological type, were not significantly related to TTI1 expression. Furthermore, univariate and multivariate analysis validated that TTI1 expression, TNM stage and lymph node metastasis were independent predictors of OS (Table 2), and TTI1 expression, TNM stage and differentiation were independent predictors of DFS (Table 3) in patients with NSCLC. In summary, these findings strongly indicated that the high expression of TTI1 was positively correlated with poor prognosis and might serve as a prognostic biomarker for patients with NSCLC.

Table 1
Correlations between TTI1 or Ki67 and clinical characteristics in 160 NSCLC patients

Clinicopathological parameters	TTI1^{Low}	TTI1^{High}	P Value	Ki67^{Low}	Ki67^{High}	P value
Age						
<60	48	45		51	42	
≥ 60	38	29	0.523	43	24	0.236
Gender						
Male	37	42		48	31	
Female	49	32	0.083	46	35	0.610
Smoking history						
smokers	30	32		36	26	
Nonsmokers	56	42	0.279	58	40	0.889
Histological type						
squamous	35	36		45	26	
adenocarcinoma	51	38	0.313	49	40	0.288
Tumor stage						
I–II	69	46		77	38	
III–IV	17	28	0.011	17	28	0.001
Lymph node metastasis						
NO	64	44		70	38	
Yes	22	30	0.044	24	28	0.025
Tumor size						
>3cm	53	30		57	26	
≥ 3cm	33	44	0.008	37	40	0.008
Differentiation						
Well and moderate	45	30		55	20	
poor	41	44	0.136	39	46	0.0004

Table 2 Univariate and Multivariate Analyses of Factors Associated with Overall Survival

Factors	OS			
	Univariate, P	Multivariate		
		HR	95% CI	P.value
Age (< 60 vs. ≥60)	0.481			NA
Gender (Female vs. male)	0.29			NA
Smoking history(Smokers vs. Nonsmokers)	0.677			NA
Histological type (SCC vs. Adenocarcinomas)	0.894			NA
Tumor stage (Ⅱ-Ⅲ vs. Ⅳ-Ⅴ)	0.004	1.717	1.062– 2.775	0.027
Lymph node metastasis(Yes vs. No)	0.005	1.66	1.025– 2.689	0.039
Tumor size (> 3cm vs. ≤3cm)	0.012			NS
Differentiation (Poor vs. Well and moderate)	0.002			NS
TTI1 expression (High vs. Low)	0.008	1.921	1.196– 3.086	0.007
KI67 expression (High vs. Low)	< 0.001	1.576	1.329– 2.152	< 0.001
TTI1 & KI67 expression (TTI1 & KI67 High vs. Others*)	< 0.001	1.727	1.298– 2.721	< 0.001
OS, Overall survival; NA, Not adopted; NS, Not significantly; SCC, Squamous cell carcinoma; 95%CI, 95% confidence interval; HR, Hazard ratio; Cox proportional hazards regression model; TTI1 & KI67 High, TTI1 ^{high} and KI67 ^{high} ; Others* (TTI1 ^{low} and KI67 ^{low} , TTI1 ^{high} and KI67 ^{low} , TTI1 ^{low} and KI67 ^{high})				

Table 3
Univariate and Multivariate Analyses of Factors Associated with Cumulative Recurrence

Cumulative Recurrence				
Factors	Multivariate			
	Univariate, P	HR	95% CI	P. value
Age (< 60 vs. ≥60)	0.952			NA
Gender (Female vs. male)	0.508			NA
Smoking history(Smokers vs. Nonsmokers)	0.431			NA
Histological type (SCC vs. Adenocarcinomas)	0.416			NA
Tumor stage (Ⅱ-Ⅲ vs. Ⅳ-Ⅴ)	0.001	1.719	1.122–2.636	0.013
Lymph node metastasis(Yes vs. No)	0.048			NS
Tumor size (> 3cm vs. ≤3cm)	0.045			NS
Differentiation (Poor vs. Well and moderate)	0.003	1.72	1.147–2.579	0.009
TTI1 expression (High vs. Low)	0.002	1.484	1.054–2.081	0.042
KI67 expression (High vs. Low)	< 0.001	1.675	1.310–2.450	0.009
TTI1 & KI67 expression (TTI1 & KI67 High vs. Others*)	< 0.001	1.395	1.067–2.137	< 0.001
OS, Overall survival; NA, Not adopted; NS, Not significantly; SCC, Squamous cell carcinoma; 95%CI, 95% confidence interval; HR, Hazard ratio; Cox proportional hazards regression model; TTI1 & KI67 High, TTI1 ^{high} and KI67 ^{high} ; Others* (TTI1 ^{low} and KI67 ^{low} , TTI1 ^{high} and KI67 ^{low} , TTI1 ^{low} and KI67 ^{high})				

TTI1 promotes NSCLC cell metastasis, invasion and proliferation in vitro

Considering the above findings, the impact of TTI1 on the biological function of NSCLC was further investigated. The mRNA and protein expression of TTI1 in HBE and 3 NSCLC cell lines was respectively detected by qRT-PCR and western blot, and the results showed that TTI1 was highly expressed in NSCLC cell lines compared with normal lung cells at both the mRNA and protein levels, and it was expressed at the highest level in A549 cells and at the lowest level in H460 cells in the 3 NSCLC cell lines (Fig. 3A, B). Thus, TTI1 was knocked down in A549 cells (A549-shTTI1) and overexpressed in H460 cells (H460-TTI1) by the lentivirus transduction method, generating two stable cell lines (Fig. 3C, D). The CCK-8 and colony formation assay showed that the proliferation ability was decreased after the knockdown of TTI1 and increased upon the upregulation of TTI1 in NSCLC cells (Fig. 3E, F). Then, the wound healing assay indicated that the migration capacity of A549-shTTI1 cells was impaired and of H460-TTI1 cells was

enhanced (Fig. 3G). Consistently, the Matrigel Transwell assay revealed that the invasion capacity of NSCLC cells in TTI1 knocked down groups was significantly reduced compared with the control group, and on the contrary, the invasion capacity was markedly improved in TTI1 upregulated group compared with the control group (Fig. 3H). Collectively, these results indicated the crucial role of TTI1 in regulating NSCLC cell growth and metastasis.

TTI1 regulates the mTOR signaling pathway and promotes NSCLC progression in vivo

Then, we further revealed the underlying mechanism by which TTI1 promotes the progression of NSCLC. Initially, we used a publicly available data (STRING, <https://cn.string-db.org/>) to find the protein-protein interaction networks about TTI1 and found that a total of 20 proteins closely interaction with TTI1 (Fig. 4A). The database had performed Kyoto Encyclopedia of Genes and Genomes (KEGG) analysis to explore TTI1-related downstream pathways and we made a bubble chart (Fig. 4B). From the KEGG analysis, we speculated that TTI1 regulates the mTOR signaling pathway in NSCLC. Hence, we detected mTOR and downstream signaling proteins, including S6K1 and 4EBP1, of NSCLC cell lines at mRNA and protein levels. We found that mTOR, S6K1, 4EBP1 of both A549-shTTI1 and H460-TTI1 had no change at mRNA and protein levels, however, p-mTOR, p-S6K1, p-4EBP1 of A549-shTTI1 was significantly reduced compared with the control group, conversely, p-mTOR, p-S6K1, p-4EBP1 of H460-TTI1 was markedly improved compared with the control group (Fig. 4C-E). Those findings elucidated that TTI1 regulates the mTOR signaling pathways in NSCLC. Finally, the in vivo assay in nude mice subcutaneously implanted with A549-shTTI1, H460-TTI1 and control cells, further identified that the knockdown of TTI1 could impaired the progression of NSCLC and the overexpression of TTI1 could accelerate the growth of NSCLC (Fig. 4F-H).

The level of TTI1 was positive correlation with the level of KI67 in NSCLC patients

We used another publicly available data (GEPIA 2 (cancer-pku.cn)) to conduct Pearson analysis of the correlation between TTI1 and KI67, and found that TTI1 and KI67 transcriptional expression had a well correlation in LUAD ($R = 0.49$, $P = 0$) and in LUSC ($R = 0.34$, $P = 1.6e-14$) (Fig. 5A). Then, TMAs of 160 NSCLC tissues were used to analyze the expression of TTI1 and KI67. According to the staining intensity of each specimen, TTI1 and KI67 expression were classified into four grades: negative, low, moderate, strong (Fig. 5B). Finally, Pearson analysis was conducted, and in accordance with before bioinformatics analysis, it had a well correlation ($R = 0.5682$, $P < 0.0001$) between TTI1 and KI67 protein expression (Fig. 5C). These findings validated that TTI1 and KI67 expression had a well correlation in NSCLC both at mRNA and protein levels.

TTI1 combined with KI67 was an independent parameter predicting the prognosis and recurrence of NSCLC patients

According to the well correlation between TTI1 and KI67, we speculated that TTI1 and KI67 together might have an influence on the prognosis of NSCLC patients. The univariate and multivariate analysis validated the expression of TTI1, the expression of KI67 and the expression of both TTI1 and KI67 were

independent predictors of OS and DFS in patients with NSCLC (Tables 2 and 3). At the last follow-up, the 2-year and 5-year OS and DFS rates of the entire population were 86%, 48.2%, 74.3%, and 35.3%, respectively. The 2- and 5-year OS and DFS rates in the TTI1 Low group was remarkably higher than those in the TTI1 High group (88.1% vs. 82.3%; 55.5% vs. 40.7%; 85.5% vs. 63.5%; 49.3% vs. 23.3%; respectively, Fig. 6A). The OS of the NSCLC KI67 low group was higher than that of the KI67 high group ($p = 0.0003$) in the 2-year and 5-year postoperative period, and the KI67 Low group of NSCLC patients with DFS was significantly higher than that of the KI67 High group ($p < 0.0001$) (Fig. 6B). Subsequently, we analyzed the combined role of TTI1 and KI67 in OS and DFS. 160 NSCLC patients were divided into 3 subgroups according to TTI1 and KI67 expression level: TTI1 high and KI67 high group, TTI1 low and KI67 low group, and others. The 2-year and 5-year OS and DFS rates in TTI1 high and KI67 high group were significantly lower than those in TTI1 low and KI67 low group and others (Fig. 6C). These findings revealed that TTI1 or KI67 could be tumour biomarker for NSCLC, however TTI1 combined with KI67 could be the better tumor biomarker for NSCLC.

Discussion

NSCLC is a devastating disease. Although the continuous improvement of treatment methods has reduced the death rate of NSCLC year by year [13], the overall cure rate and survival rate of patients with NSCLC are still very low [14]. Therefore, further exploration the mechanism of NSCLC oncogenesis, progression, and recurrence is necessary and exigent. Our study showed that TTI1 was significantly high expression in NSCLC specimens compared with non-cancerous tissues, and high TTI1 expression was positively associated with large tumor size, advanced TNM stage and lymph node metastasis. Furthermore, patients with high expression of TTI1 and KI67 had poor prognosis and high recurrence than those with low level of TTI1 and KI67. Importantly, we found that the combination of TTI1 and KI67 was an independent parameter for predicting prognosis and recurrence in NSCLC patients. On this basis, we conclude that TTI1 serves as the facilitator of NSCLC progression, and TTI1 or TTI1 combined with KI67 can be used to predict prognosis and recurrence in patients with NSCLC.

The TELO2-TTI1-TTI2 (TTT) complex can recognize newly synthesized PIKKs and transfer them to the R2TP complex (RUVBL1-RUVBL2-RPAP3-PIH1D1) and heat shock protein 90 (HSP-90) chaperone to support their folding and assembly [4, 5]. As a member of the Ser/Thr kinase family, Phosphatidylinositol 3-kinase-related protein kinases (PIKKs) play pivotal roles in various pathways related to cell metabolism, proliferation, and differentiation. All three proteins of TTT complex form elongated helical repeat structures. TTI1 provides a platform on which TELO2 and TTI2 bind to its central region and C-terminal end, respectively [15]. Therefore, TTI1 is a critical element for maintaining the stability and function of the TTT complex. TTI1 and TTI2 are also required for maintaining the protein levels of TEL2, and the triple T complex is required for DNA damage response (DDR) signaling through control of the protein levels of ataxia telangiectasia-mutated (ATM), ataxia-telangiectasia and Rad3-related (ATR), and a group of related PIKKs. Thereinto, TTI1 plays a pivotal role for DNA damage resistance, and studies prove that TTI1 depletion led to significant DNA damage sensitivity [16].

The activated mTOR signaling pathway is the key to promoting cell growth, and plays a variety of roles in human cancer, including cell survival, cytoskeleton rearrangement, invasion, metastasis, anti-apoptosis, and inhibition of autophagy[6, 17–19]. Recent studies have indicated that activated mTOR signaling could promote cancer cell proliferation, invasion and metastasis[20–22]. Kangsan Kim et found that augmented mTORC1 signaling determines metastatic potential in renal cell carcinoma[22]. TTI1 and TTI2 are important for mTOR stability to maintain its activities.

Our study validated that overexpression of TTI1 could promote NSCLC cell proliferation, invasion and metastasis in vitro, and boosted NSCLC cell progression in vivo. However, the opposite result was obtained in NSCLC cells of TTI1 knockdown. Mechanistically, overexpression of TTI1 promotes phosphorylation of mTOR, S6K1 and 4EBP1. However, after the TTI1 was knocked down, the levels of p-mTOR, p-S6K1 and p-4EBP1 decreased in NSCLC cells. Thus, our date revealed that TTI1 could regulate mTOR signaling activities. This explains that TTI1 can promote NSCLC proliferation, invasion and metastasis. Moreover, TTI1 is positively associated with the expression of KI67 in NSCLC tissues, and it is proved that TTI1 promotes NSCLC development via facilitating cell proliferation from another aspect.

Conclusion

These findings of our study suggested a pivotal oncogenic role of TTI1 in the progression of NSCLC and demonstrated an independent prognostic role of TTI1 in NSCLC. In terms of mechanism, TTI1 could regulate the mTOR signaling pathway. The expression of TTI1 and KI67 had a well correlation in NSCLC and combination of TTI1 and KI67 is a valuable biomarker for predicting the survival and recurrence of patients with NSCLC.

Abbreviations

NSCLC, non-small-cell lung cancer; LUAD, lung adenocarcinomas; LUSC, squamous cell carcinomas; TCGA, The Cancer Genome Atlas; GEO, Gene Expression Omnibus; qRT-PCR, quantitative real-time polymerase chain reaction; IHC, immunohistochemistry; CCK-8, cell counting kit-8; OS, overall survival; DFS, Disease free survival; FP, First progression; PPS, Post progression survival; TTI1, TELO2-interacting protein 1; S6K1, ribosomal protein S6 kinase beta-1.

Declarations

Acknowledgments

None.

Authors' contributions

S-Q Z, L-X Z and X Y conceived and designed the experiments; L-X Z, X Y and Z-B W performed the experiments; Z-M L, D-G W, S-W C, F L and Y-B W analyzed the data; L-X Z and X Y wrote the paper. All

authors have read and approved the final manuscript.

Funding

This work was supported by the following grants: National Natural Science Foundation of China (81860520); Department of Science and Technology of Jiangxi Province (20213BCJL22048).

Availability of data and materials

All data in our study are available upon request.

Ethics approval and consent to participate

The ethical approval was provided by the Ethics Committee of the Second Affiliated Hospital of Nanchang University, and written informed consent was obtained from each patient.

Consent for publication

Not applicable.

Competing interests

None.

References

1. Sung, H., et al., Global Cancer Statistics 2020: GLOBOCAN Estimates of Incidence and Mortality Worldwide for 36 Cancers in 185 Countries. *CA Cancer J Clin*, 2021. 71(3): p. 209–249.
2. Ettinger, D.S., et al., Non-Small Cell Lung Cancer, Version 5.2017, NCCN Clinical Practice Guidelines in Oncology. *J Natl Compr Canc Netw*, 2017. 15(4): p. 504–535.
3. Molina, J.R., et al., Non-small cell lung cancer: epidemiology, risk factors, treatment, and survivorship. *Mayo Clin Proc*, 2008. 83(5): p. 584 – 94.
4. Pal, M., et al., Structure of the TELO2-TTI1-TTI2 complex and its function in TOR recruitment to the R2TP chaperone. *Cell Rep*, 2021. 36(1): p. 109317.
5. Takai, H., et al., Tel2 structure and function in the Hsp90-dependent maturation of mTOR and ATR complexes. *Genes Dev*, 2010. 24(18): p. 2019-30.
6. Murugan, A.K., mTOR: Role in cancer, metastasis and drug resistance. *Semin Cancer Biol*, 2019. 59: p. 92–111.
7. Kaizuka, T., et al., Tti1 and Tel2 are critical factors in mammalian target of rapamycin complex assembly. *J Biol Chem*, 2010. 285(26): p. 20109-16.
8. Rao, F., et al., Inositol pyrophosphates mediate the DNA-PK/ATM-p53 cell death pathway by regulating CK2 phosphorylation of Tti1/Tel2. *Mol Cell*, 2014. 54(1): p. 119–132.

9. Fernández-Sáiz, V., et al., SCFFbxo9 and CK2 direct the cellular response to growth factor withdrawal via Tel2/Tti1 degradation and promote survival in multiple myeloma. *Nat Cell Biol*, 2013. 15(1): p. 72–81.
10. Pei, X., et al., circMET promotes NSCLC cell proliferation, metastasis, and immune evasion by regulating the miR-145-5p/CXCL3 axis. *Aging (Albany NY)*, 2020. 12(13): p. 13038–13058.
11. Qiu, B.Q., et al., CircRNA fibroblast growth factor receptor 3 promotes tumor progression in non-small cell lung cancer by regulating Galectin-1-AKT/ERK1/2 signaling. *J Cell Physiol*, 2019. 234(7): p. 11256–11264.
12. Camp, R.L., M. Dolled-Filhart and D.L. Rimm, X-tile: a new bio-informatics tool for biomarker assessment and outcome-based cut-point optimization. *Clin Cancer Res*, 2004. 10(21): p. 7252-9.
13. Siegel, R.L., et al., Cancer Statistics, 2021. *CA Cancer J Clin*, 2021. 71(1): p. 7–33.
14. Hirsch, F.R., et al., Lung cancer: current therapies and new targeted treatments. *Lancet*, 2017. 389(10066): p. 299–311.
15. Kim, Y., et al., Structure of the Human Telo2-Tti1-Tti2 Complex. *J Mol Biol*, 2021. 434(2): p. 167370.
16. Hurov, K.E., C. Cotta-Ramusino and S.J. Elledge, A genetic screen identifies the Triple T complex required for DNA damage signaling and ATM and ATR stability. *Genes Dev*, 2010. 24(17): p. 1939-50.
17. Wullschleger, S., R. Loewith and M.N. Hall, TOR signaling in growth and metabolism. *Cell*, 2006. 124(3): p. 471 – 84.
18. Mossmann, D., S. Park and M.N. Hall, mTOR signalling and cellular metabolism are mutual determinants in cancer. *Nat Rev Cancer*, 2018. 18(12): p. 744–757.
19. Zhou, H. and S. Huang, Role of mTOR signaling in tumor cell motility, invasion and metastasis. *Curr Protein Pept Sci*, 2011. 12(1): p. 30–42.
20. Zhang, X., et al., Circular RNA circNRIP1 acts as a microRNA-149-5p sponge to promote gastric cancer progression via the AKT1/mTOR pathway. *Mol Cancer*, 2019. 18(1): p. 20.
21. Yang, C., et al., Tumor-derived exosomal microRNA-106b-5p activates EMT-cancer cell and M2-subtype TAM interaction to facilitate CRC metastasis. *Mol Ther*, 2021. 29(6): p. 2088–2107.
22. Kim, K., et al., Determinants of renal cell carcinoma invasion and metastatic competence. *Nat Commun*, 2021. 12(1): p. 5760.

Figures

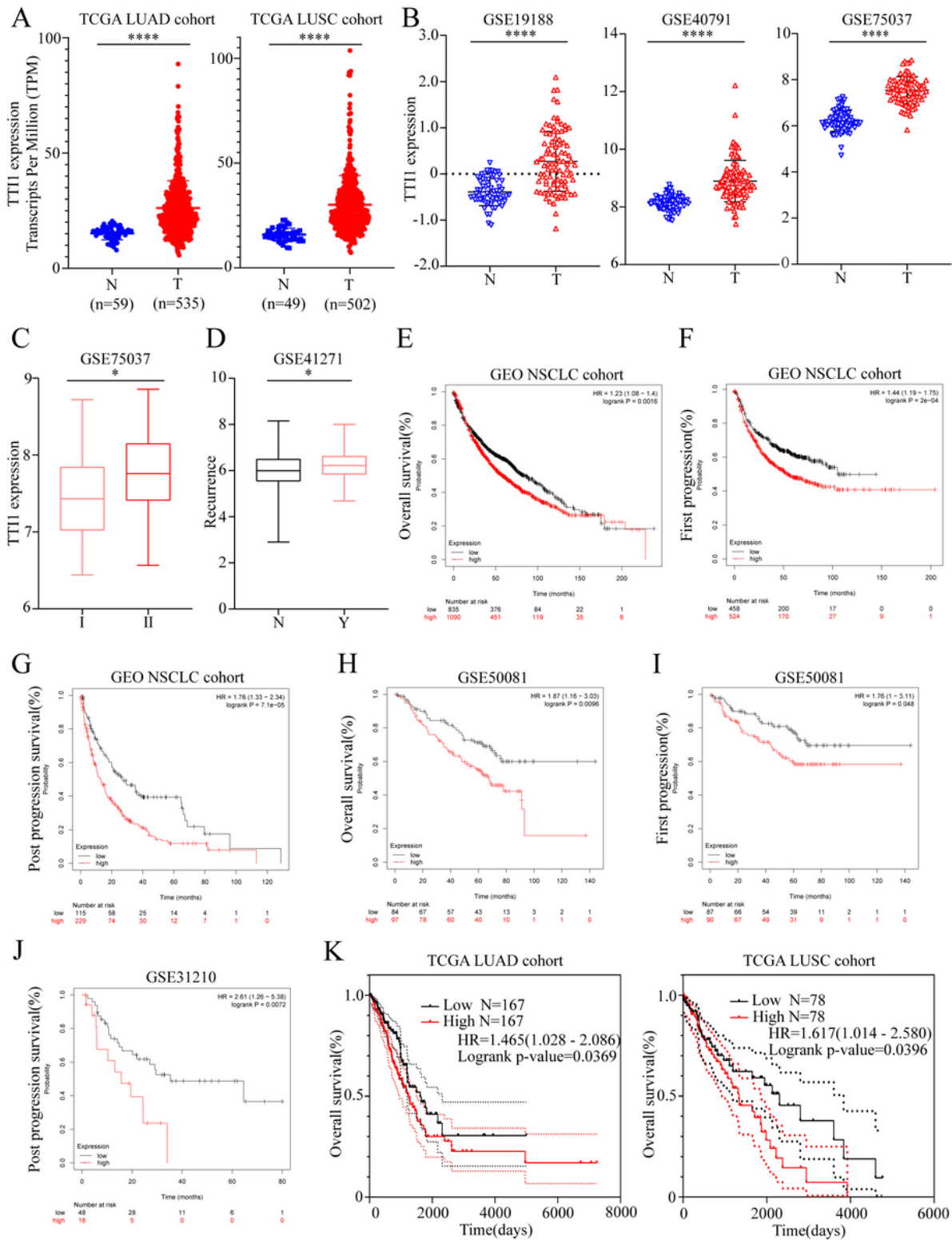


Figure 1

Expression of TTI1 mRNA in NSCLC and its prognostic significance based on bioinformatic analysis.

(a) Expression levels of TTI1 was analyzed in LUAD and LUSC tissues from TCGA databases.

(b) Expression of TTI1 in three independent GEO datasets.

(c) Expression of TTI1 respectively in \square , \square clinically TNM stage.

(d) Expression of TTI1 separately in no or yes recurrence.

(e) Overall survival (OS), (f) First progression (FP) and (g) Post progression survival (PPS) rates analysis of the NSCLC patients based on GEO databases.

(h) OS, (i) FP and (j) PPS rates analysis of the NSCLC patients in GSE50081, GSE31210. (K) OS rates analysis of the LUAD and LUSC patients based on TCGA databases.

Data are presented as the means \pm SD. * $p < 0.05$, **** $p < 0.0001$.

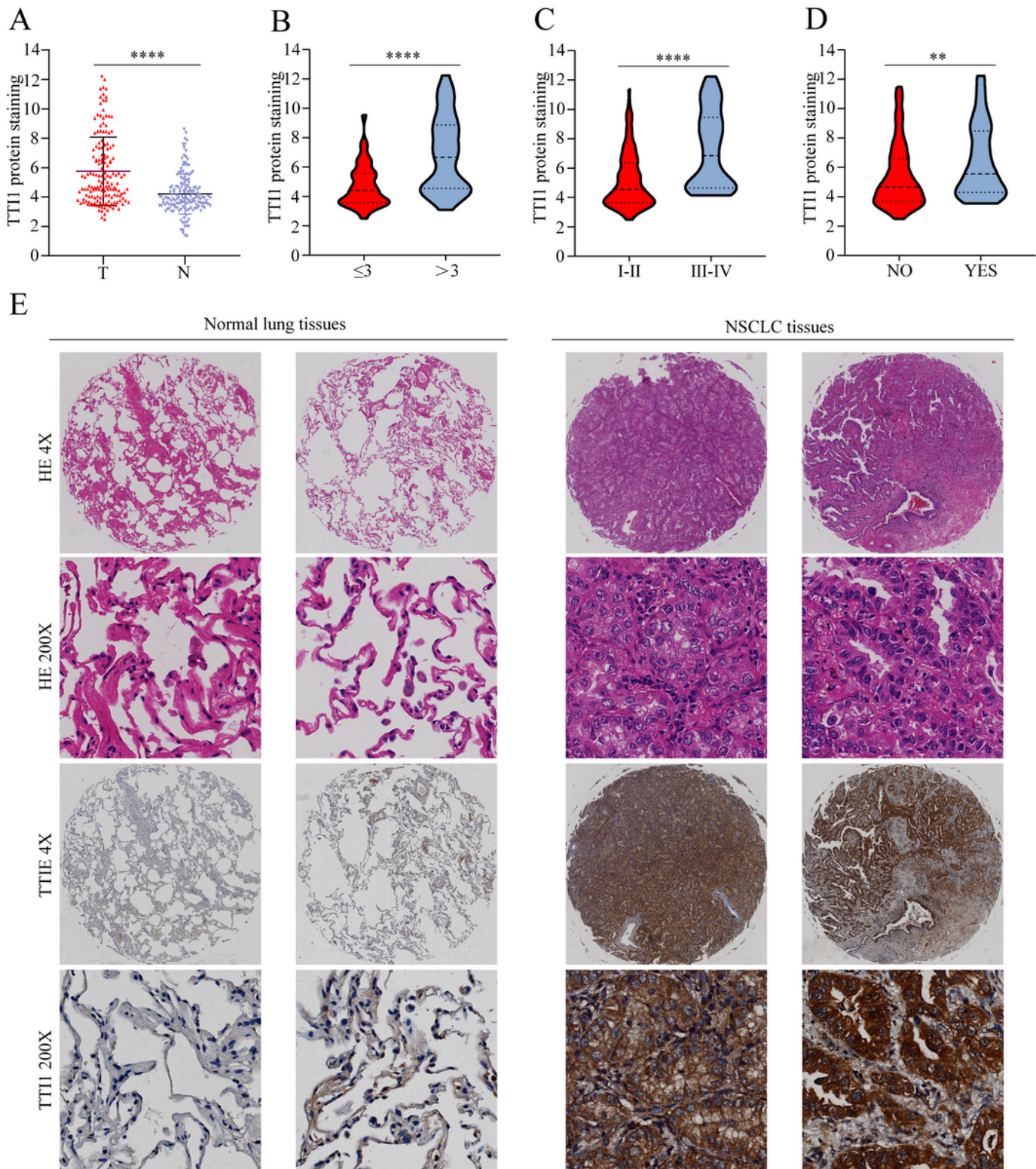


Figure 2

Expression of TTI1 protein level and its association with malignant phenotypes in NSCLC patients.

(a) Expression of TTI1 protein level in NSCLC tissues and non-cancerous tissues.

(b), (c) and (d) The expression of TTI1 was analyzed according to the tumor diameter (≤ 3 cm vs. > 3 cm), TNM stage (I-II vs. III-IV) and lymph node metastasis status (yes vs. no).

(e) Representative images of TTI1 expression in NSCLC tissues of serial sections stained with H&E and IHC.

Data are presented as the means \pm SD of three independent experiments. ** $p < 0.01$, **** $p < 0.0001$.

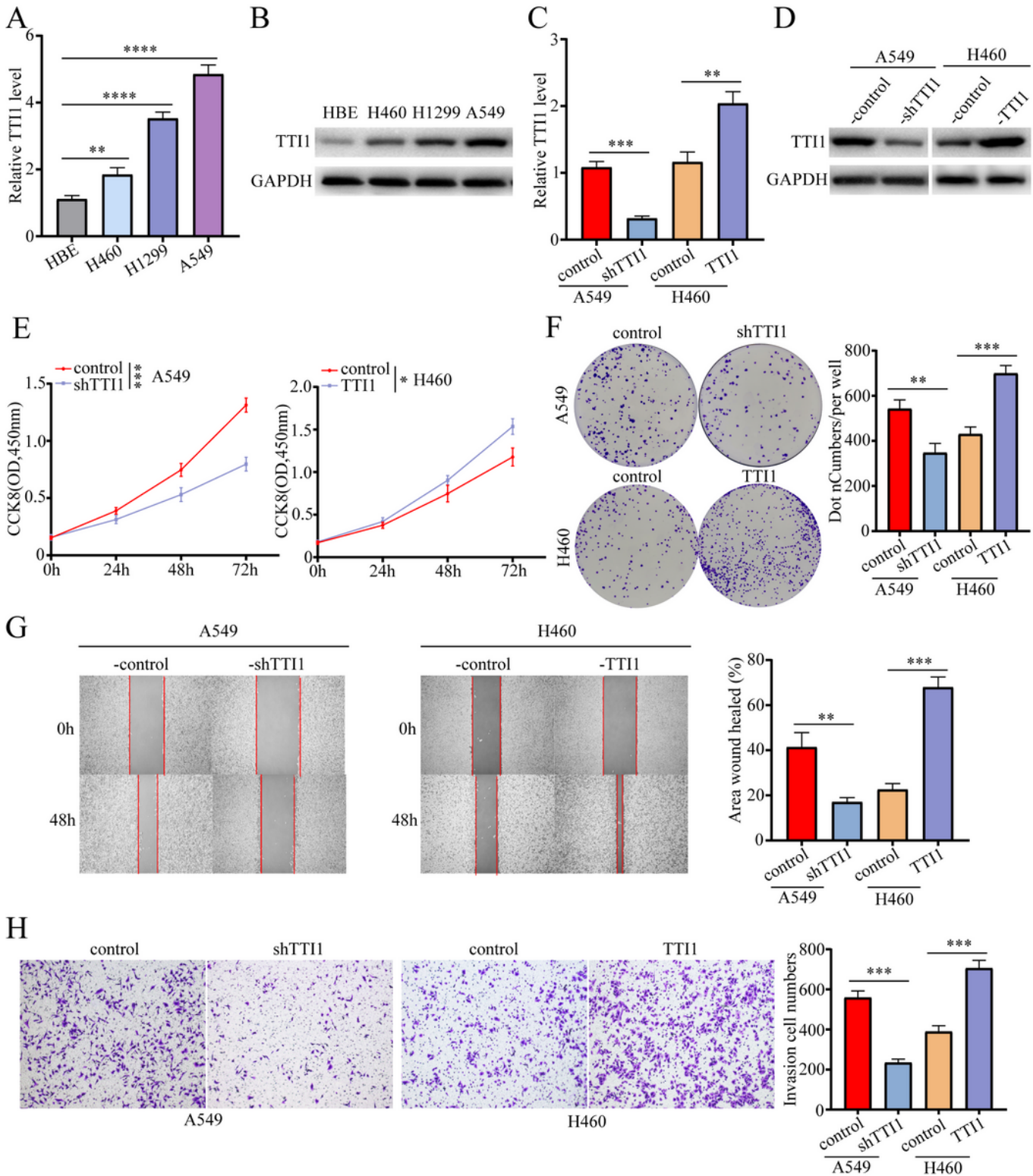


Figure 3

TTI1 knockdown or overexpression could alter the invasion, metastasis and the proliferation of NSCLC cell in vitro.

(a), (b) The mRNA and protein expression levels of TTI1 in HBE and 3 NSCLC cell lines (H460, A549 and H1299) was detected respectively by qRT-PCR and western blot.

(c), (d) The transfection efficiency of two stable cell lines, H460-TTI1 and A549-shTTI1, was validated by qRT-PCR and western blot.

(e) The proliferation ability of H460-TTI1 and A549-shTTI1 cells was measured by CCK-8 assay.

(f) The viability of H460-TTI1 and A549-shTTI1 cells was detected by colony formation assays.

(g) The migration of H460-TTI1 and A549-shTTI1 cells was detected by wound healing assay.

(h) The invasion ability of H460-TTI1 and A549-shTTI1 cells was detected by Matrigel Transwell assay.

Data are presented as the means \pm SD; n=3, **p < 0.01, ***p < 0.01, ****p < 0.0001.

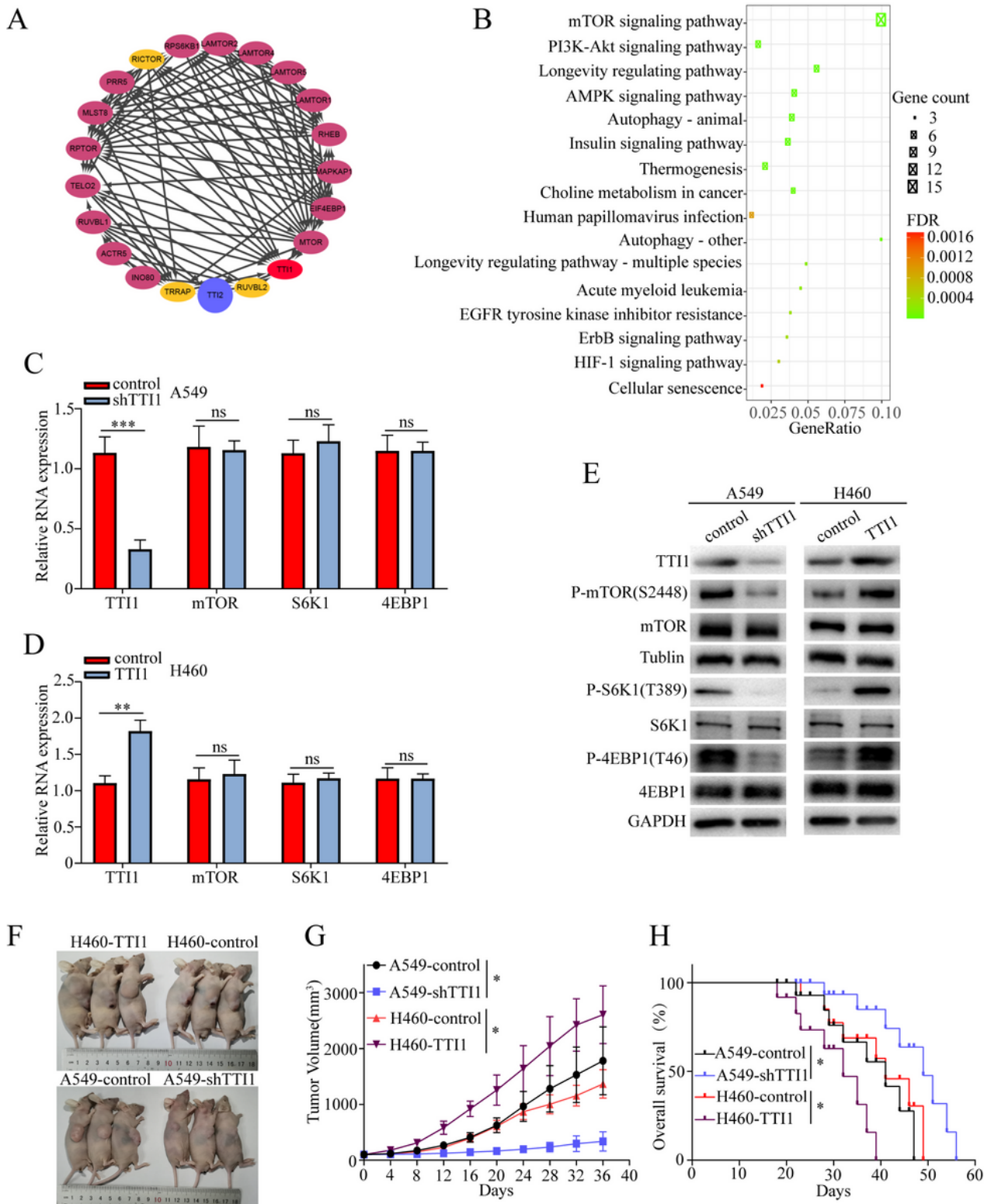


Figure 4

TTI1 regulates the mTOR signaling pathway and promotes NSCLC progression in vivo

(a) Protein-protein interaction networks about TTI1 from the STRING database.

(b) Kyoto Encyclopedia of Genes and Genomes (KEGG) analysis to explore TTI1-related downstream pathways from the STRING database.

(c), (d) qRT-PCR detects TTI1, mTOR, and downstream signaling genes mRNA levels, including S6K1, 4EBP1.

(e) Western blot analyzed TTI1, mTOR, p-mTOR, S6K1, p-S6K1 and 4EBP1, p-4EBP1 protein levels.

(f) Image of Harvested subcutaneous tumors that A549-shTTI1, H460-TTI1, and negative control cells were implanted into the nude mice.

(g) Tumor volume was calculated every 4 days after they reached 100mm³.

(h) The prognosis of the nude mice subcutaneously implanted with A549-shTTI1, H460-TTI1, and negative control cells.

Data are presented as the means \pm SD; n=3, *p < 0.05, **p < 0.01, ***p < 0.001, ns: not significant

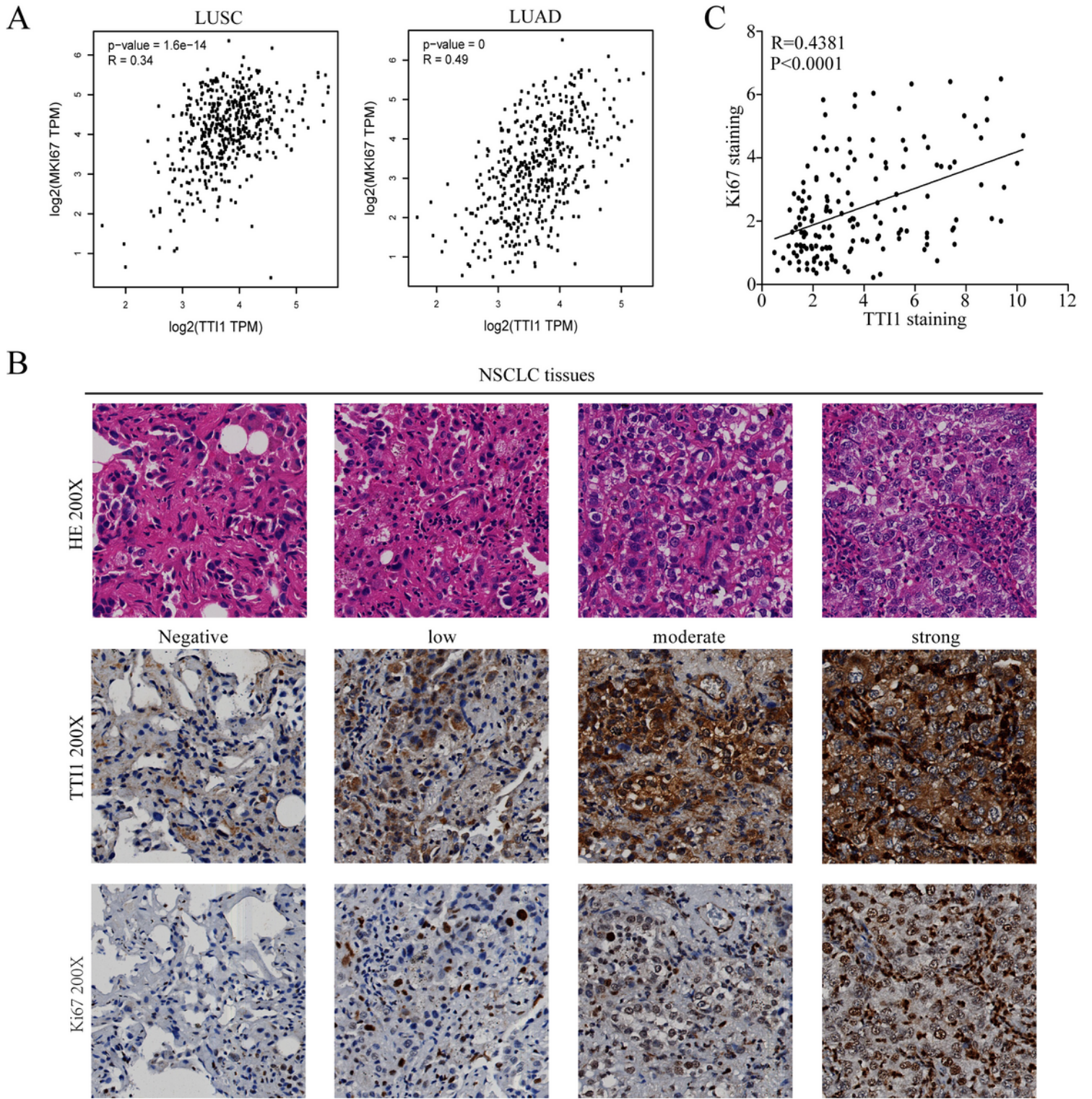


Figure 5

The expression of TTI1 and Ki67 in NSCLC patients.

(a) Pearson analysis of the correlation between TTI1 and Ki67 were conducted on GEPIA which all data based on TCGA.

(b) Representative images of TTI1 and Ki67 expression in NSCLC tissues of serial sections stained with H&E and IHC.

(c) Pearson analysis of the correlation between TTI1 and Ki67 expression in 160 paired NSCLC specimens.

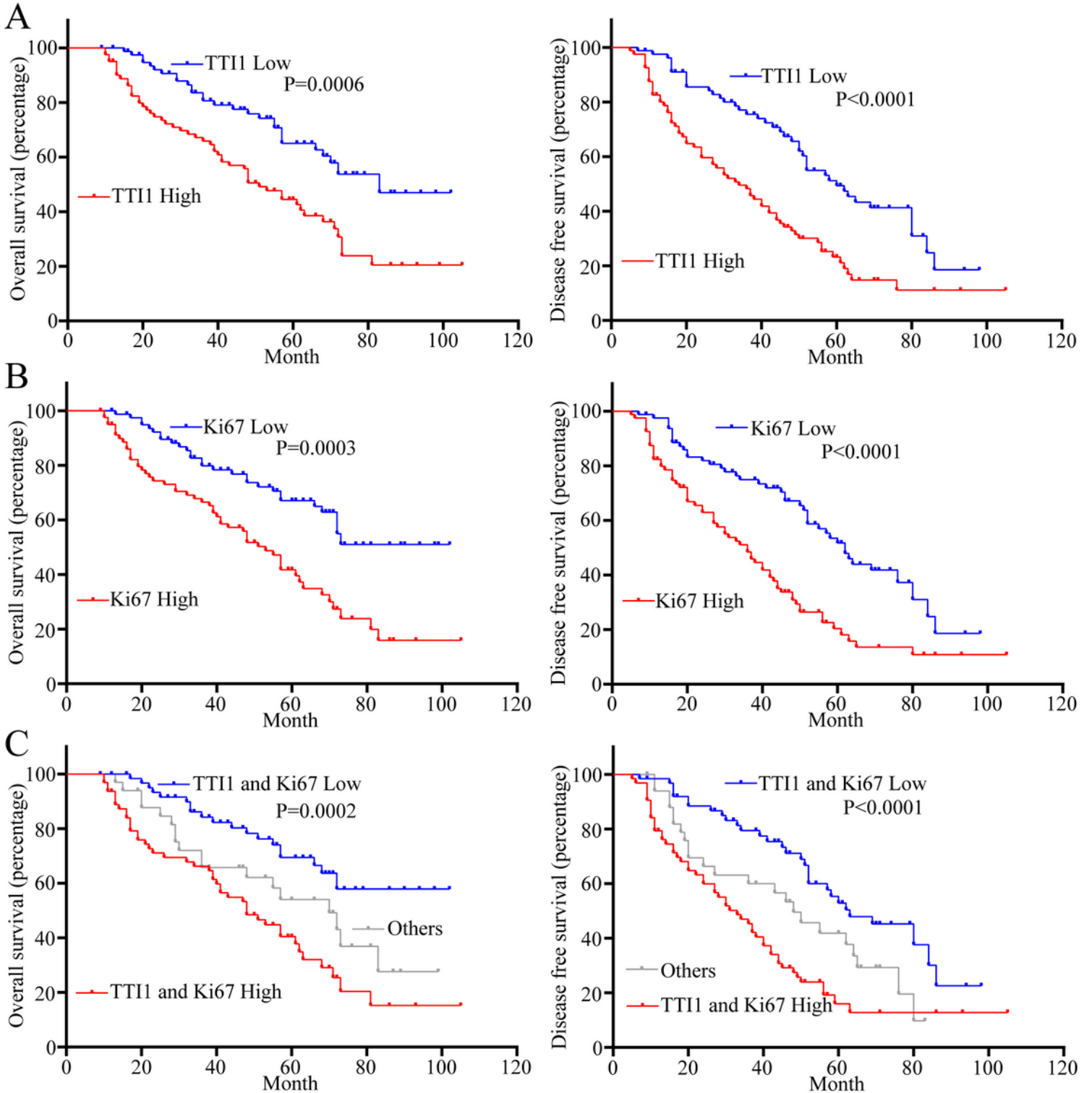


Figure 6

Prognostic significance of TTI1 and KI67 in NSCLC patients.

- (a) Survival analysis of OS and DFS of 160 NSCLC patient groups according to the expression of TTI1 (TTI1^{high} vs. TTI1^{low}) was performed using Kaplan-Meier and log rank analysis.
- (b) Survival analysis of OS and DFS of 160 NSCLC patients groups according to the expression of KI67 (KI67^{high} vs. KI67^{low}).
- (c) Survival analysis of OS and DFS of 160 NSCLC patient groups according to the expression of TTI1 and KI67 (TTI1 and KI67 high vs. TTI1 and KI67 low vs. others).

OS: Overall survival, DFS: Disease free survival.